New Phytologist

***New Phytologist* Supporting Information**

Article title: Physiological roles of Casparian strips and suberin in the transport of water and solutes.

Authors: Monica Calvo-Polanco, Zoe Ribeyre, Myriam Dauzat, Guilhem Reyt, Christopher Hidalgo-Shrestha, Patrick Diehl, Marc Frenger, Thierry Simonneau, Bertrand Muller, David E Salt, Rochus B Franke, Christophe Maurel, Yann Boursiac

Article acceptance date: 02 August 2021

The following Supporting Information is available for this article:

Fig. S1 Initial characterization of new enhanced suberin mutants. Screening of insertion mutants and suberin monomer analysis.
Fig. S2 Propidium iodide penetration in the root of CS and suberin mutants.
Fig. S3 Deconvolution of the Auramine O signal in 21d hydroponically grown plants enables the detection and quantification of endodermal and peridermal suberin.
Fig. S4 Correlations between root hydraulic conductivity ($Lp_{r\text{-}h}$) and PIP aquaporins expression levels.
Fig. S5 Effect of NaCl on the root hydraulic conductivity ($Lp_{r\text{-}h}$) of Col-0 and of a collection of 16 CS and suberin mutants.
Fig. S6 Kinetics of rosette development and transpiration rates in Col-0 and in a selection of CS and suberin mutants.
Table S1 Table summarizing the different mutants analyzed in the present study.
Table S2 Ionomic comparisons of the shoots of CS and suberin deficient mutants.

Fig S1 Initial characterization of new enhanced suberin mutants. Screening of insertion mutants and suberin monomer analysis.

(a) eFP visualization of the root expression pattern of the GDSL-like lipase/hydrolase gene *GELP51* (*At2g23540*). Display of absolute expression values for *GELP51* in the root. Consistent with a putative function on root suberization *GELP51* is predominantly expressed in the endodermis. Data and graphics were extracted from the Arabidopsis Translatome eFP Browser available at http://bar.utoronto.ca (Mustroph et al., 2009).

(b) Schematic drawing of the GELP51 locus (At2g23540) with indicated T-DNA insertion positions of available mutant line's (GK_016A11, *gelp51-2*; SALK_033359, *gelp51-1*).

(c) Semi-quantitative RT-PCR on the GK_016A11 line, SALK_033359 line and on Col-0 plants for *GELP51* transcript levels in roots. *ACTIN* was used as internal control. Line GK_016A11, now named *gelp51-2*, was selected for further analysis.

(d) GC-MS quantification of the suberin monomer profiles of *gelp51-2* and wildtype Col-0 roots following delipidation and depolymerization according to Franke et al., 2005. The *gelp51-2* mutant is substantially increased in the predominant suberin monomers. The total suberin content in *gelp51-1* is 39% higher compared to the wildtype (Figure 1)[1]. ω-OH-Acids, ω-Hydroxyacids; α,ω-Diacids, α,ω-Dicarboxylic acids. Data are means ± SD, n=6. Significances relative to wildtype (t-test, *P<0.05, **P<0.01).

(e) eFP visualization of the root expression pattern of the NAC-like transcription factor gene *ANAC038* (*At2g24430*). Display of absolute expression values for *ANAC038* in the root. Consistent with a putative function on root suberization *ANAC038* is predominantly expressed in the endodermis. Data and graphics were extracted from the Arabidopsis Translatome eFP Browser.

(f) Schematic drawing of the ANAC038 locus (At2g24430) with indicated T-DNA insertion positions of available mutant line's with the selected mutant line's (GK_890E11; FLAG_335C06; SAIL_784G11; SALK_103716, *anac038-1*; WiscDsLox_HS007-11H, *anac038-2*).

(g) Semi-quantitative RT-PCR screening on the insertion lines FLAG_335C06, GK_890E11, SAIL_784G11, SALK_103716, WiscDsLox_HS007-11H and on Col-0 plants for *ANAC038* transcript levels in roots. *ACTIN* was used as internal control. Lines FLAG_335C06, GK_890E11 and SAIL_784G11 did not show any significant changes in *ANAC038* expression levels. Mutant lines SALK_103716, now named *anac038-1*, and WiscDsLox_HS007-11H, now named *anac038-2*, were characterized as transcriptional knock-out mutants and selected for subsequent suberin analysis by GC-MS.

(h) GC-MS quantification of the suberin monomer profiles of *anac038-1* and wildtype Col-0 roots as in (d). The *anac038-1* mutant is significantly increased in all aliphatic suberin monomers. The total suberin content in *anac038-1* is 31% higher compared to the wildtype (Figure 1C). The *anac038-2* mutant from the WiscDsLox T-DNA collection showed a very similar increased suberin phenotype[2]. As the majority of the mutants used in this study were from the SALK collection, *anac038-1* was selected for the physiological studies. ω-OH-Acids, ω-Hydroxyacids; α,ω-Diacids, α,ω-Dicarboxylic acids. Data are means ± SD, n=6. Significances relative to wildtype (t-test, *P<0.05, **P<0.01).

(i) GC-MS quantification of the suberin monomer profiles of *anac038-2* and wildtype Col-0 roots as in (D). The *anac038-2* mutant is significantly increased in the all suberin monomers. The total suberin content in *anac038-2* is 43% higher compared to the wildtype (Figure 1C). The *anac038-2* mutant is from the WiscDsLox T-DNA collection (Woody et al., 2006). As the majority of the mutants used in this study were from the SALK collection, *anac038-2* was not included in all studies. ω-OH-Acids, ω-Hydroxyacids; α,ω-Diacids, α,ω-Dicarboxylic acids. Data are means ± SD, n=4. Significances relative to wildtype (t-test, *P<0.05, **P<0.01).

[1] Albeit endodermis specific GELP51 expression, GELP51 co-oexpression with known suberin genes and the enhanced root suberin content in the line GK_016A11 we do not want to claim that these data are prove for GELP51 being required for suberin formation. It is relevant for this study that line GK_016A11, named *gelp51-2*, consistently shows an enhanced root suberin content. An in-depth characterization of these mutants and the mutated genes will be published separately.

[2] An in-depth characterization of these mutants and the mutated genes will be published separately.

Primers:
For semiquantitative RT-PCR of *GELP51:*
LS832 GGCGGATTAGGAGCTTCTTT
LS833 AACAAGCCTTTGTCGCACTT

For semiquantitative RT-PCR of *ANA038:*
LS908 CGAAAATGGGAGGAAAAGAA
LS839 CGCCATTGTACGAAGCACTA

At2g23540 (GELP51)

(a)

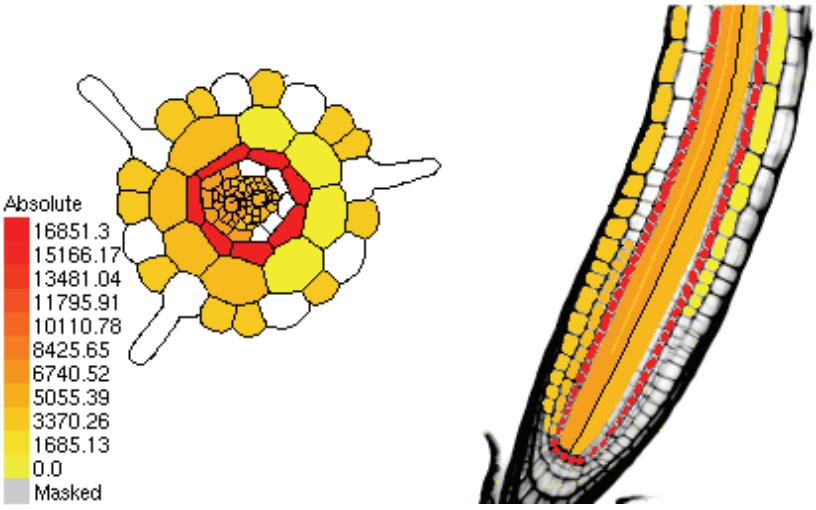

(b)

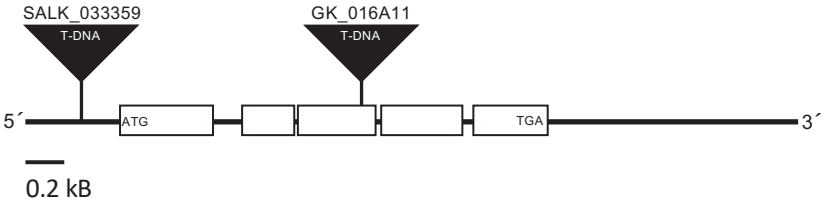

(c)

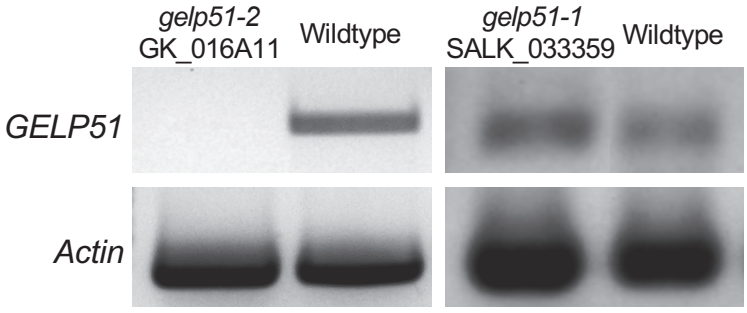

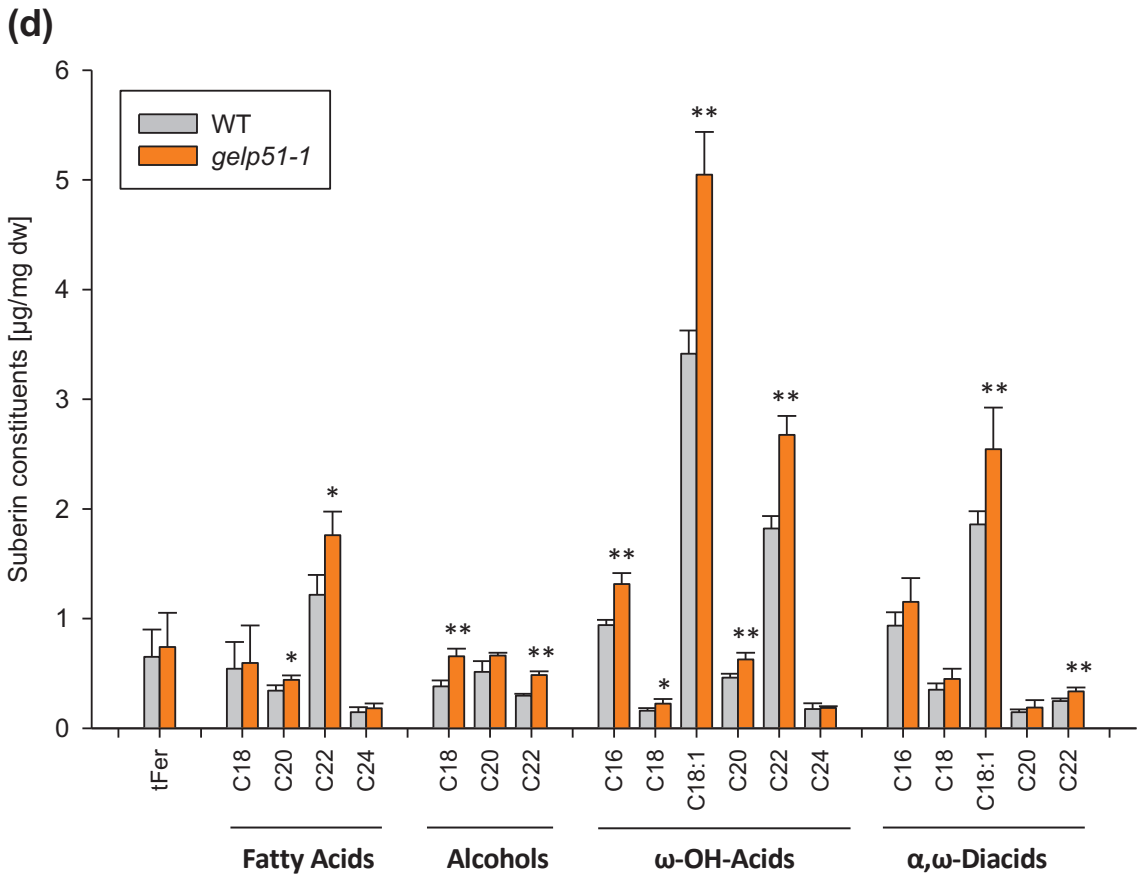
(d)
WT
gelp51-1
Suberin constituents [µg/mg dw]
0
1
2
3
4
5
6
tFer
C18
C20
C22
C24
C18
C20
C22
C16
C18
C18:1
C20
C22
C24
C16
C18
C18:1
C20
C22
Fatty Acids
Alcohols
ω-OH-Acids
α,ω-Diacids

At2g24430 (ANAC038)

(e)

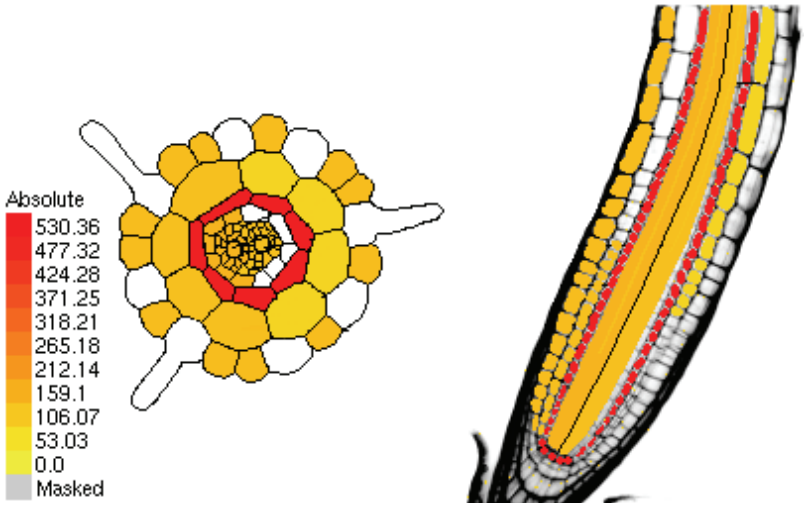

(f)

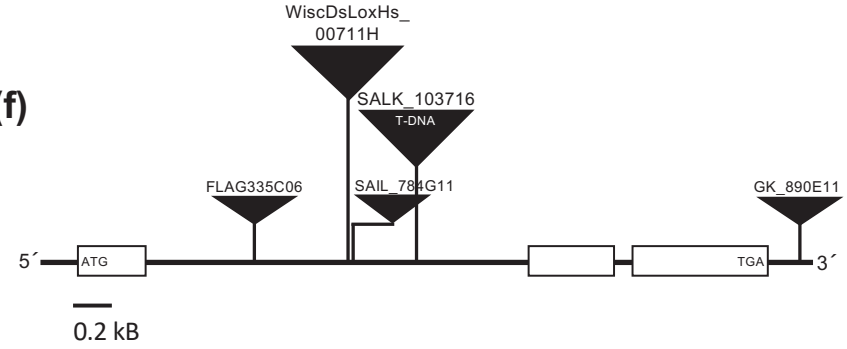

(g)

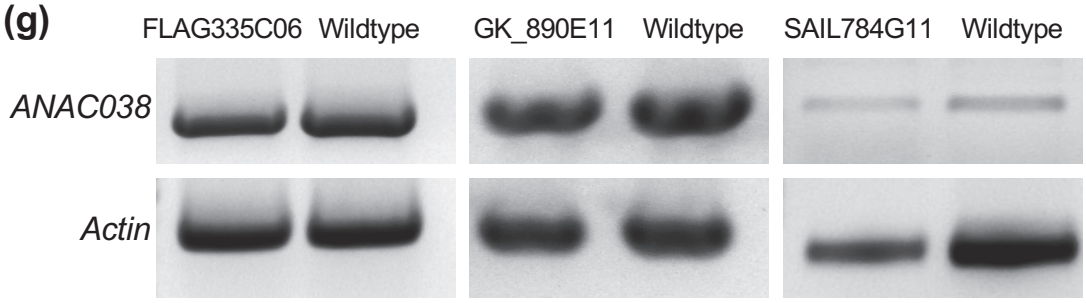

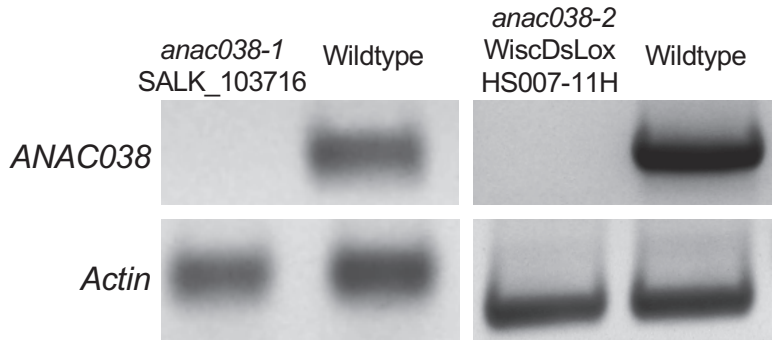

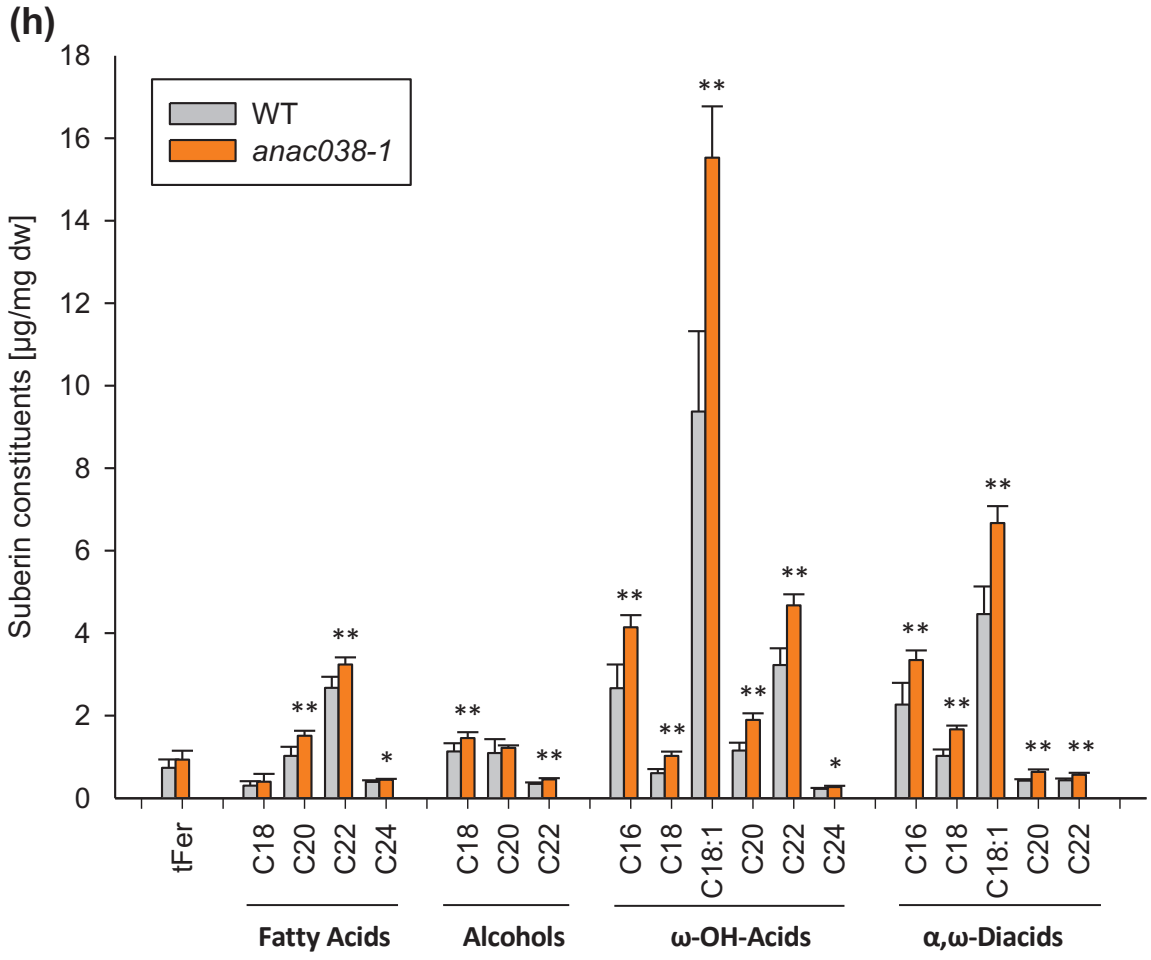
(h)
WT
anac038-1
Suberin constituents [µg/mg dw]
0
2
4
6
8
10
12
14
16
18
tFer
C18
C20
C22
C24
C18
C20
C22
C16
C18
C18:1
C20
C22
C24
C16
C18
C18:1
C20
C22
Fatty Acids
Alcohols
ω-OH-Acids
α,ω-Diacids

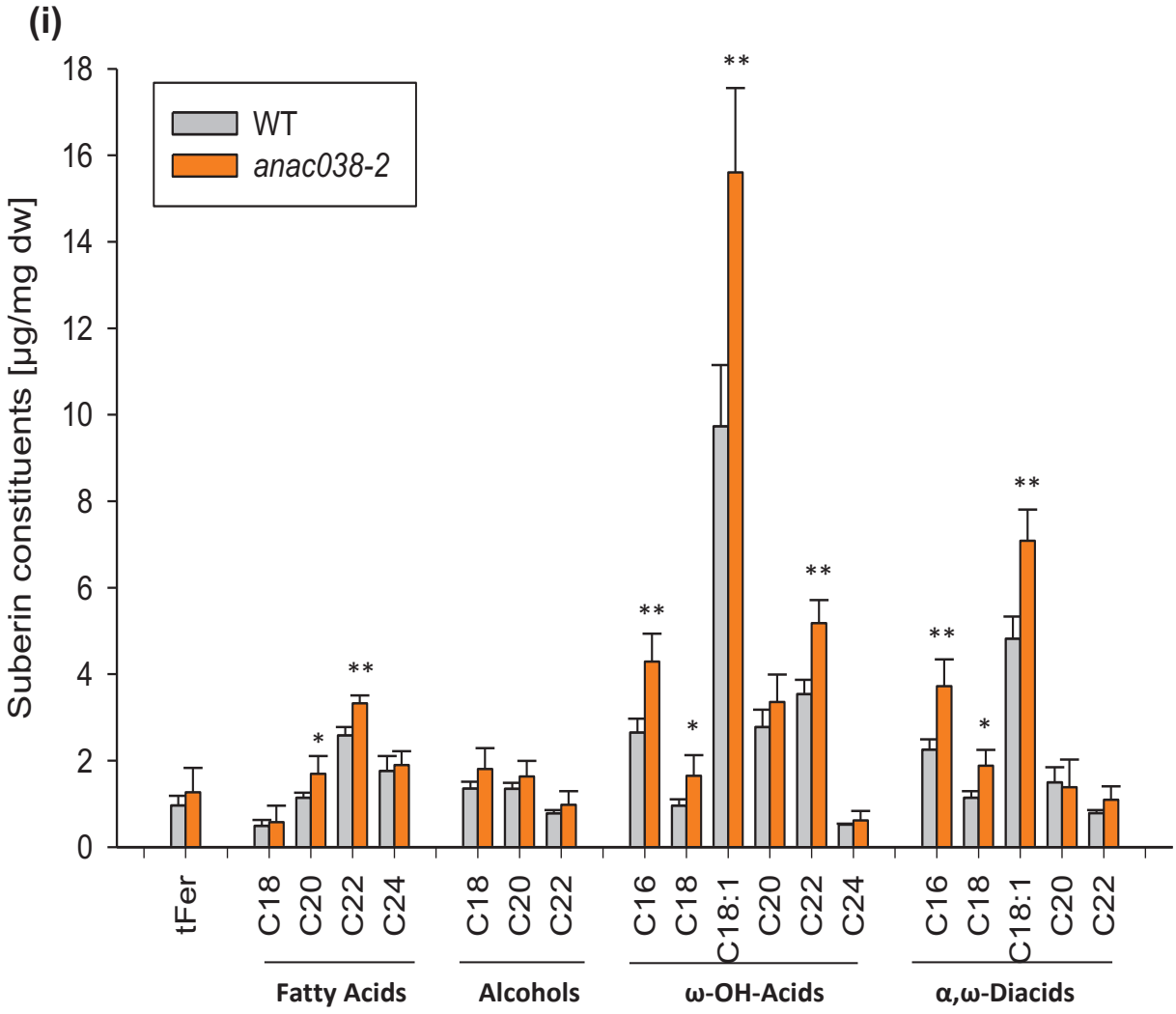
(i)
Suberin constituents [µg/mg dw]
WT
anac038-2
tFer
C18
C20
C22
C24
C18
C20
C22
C16
C18
C18:1
C20
C22
C24
C16
C18
C18:1
C20
C22
Fatty Acids
Alcohols
ω-OH-Acids
α,ω-Diacids

Fig. S2 Propidium iodide penetration in the root of CS and suberin mutants. Confocal cross-section of PI stained 21 days-old plants at various locations along the root, as indicated in Figure **1a**. Asterisks mark the staining of the xylem vessels after penetration of the PI into the stele. In magenta: primary root. In red: lateral roots. One representative image is shown, n ≥ 3. Scale bar = 50µm. Method: 21 days-old plants cultivated for 10 days in vitro and then 11 days in hydroponics were incubated for 1h in 2ml of 1/1000 propidium iodide in hydroponic solution. Cross-sections were reconstructed from Leica SP8 confocal z-stack images. Imaging parameters were identical for all images: 40x water objective, excitation: 633nm from HeNe laser with z-correction 2-8% intensity, emission: 723-730nm.

New Phytologist

PRIMARY ROOT

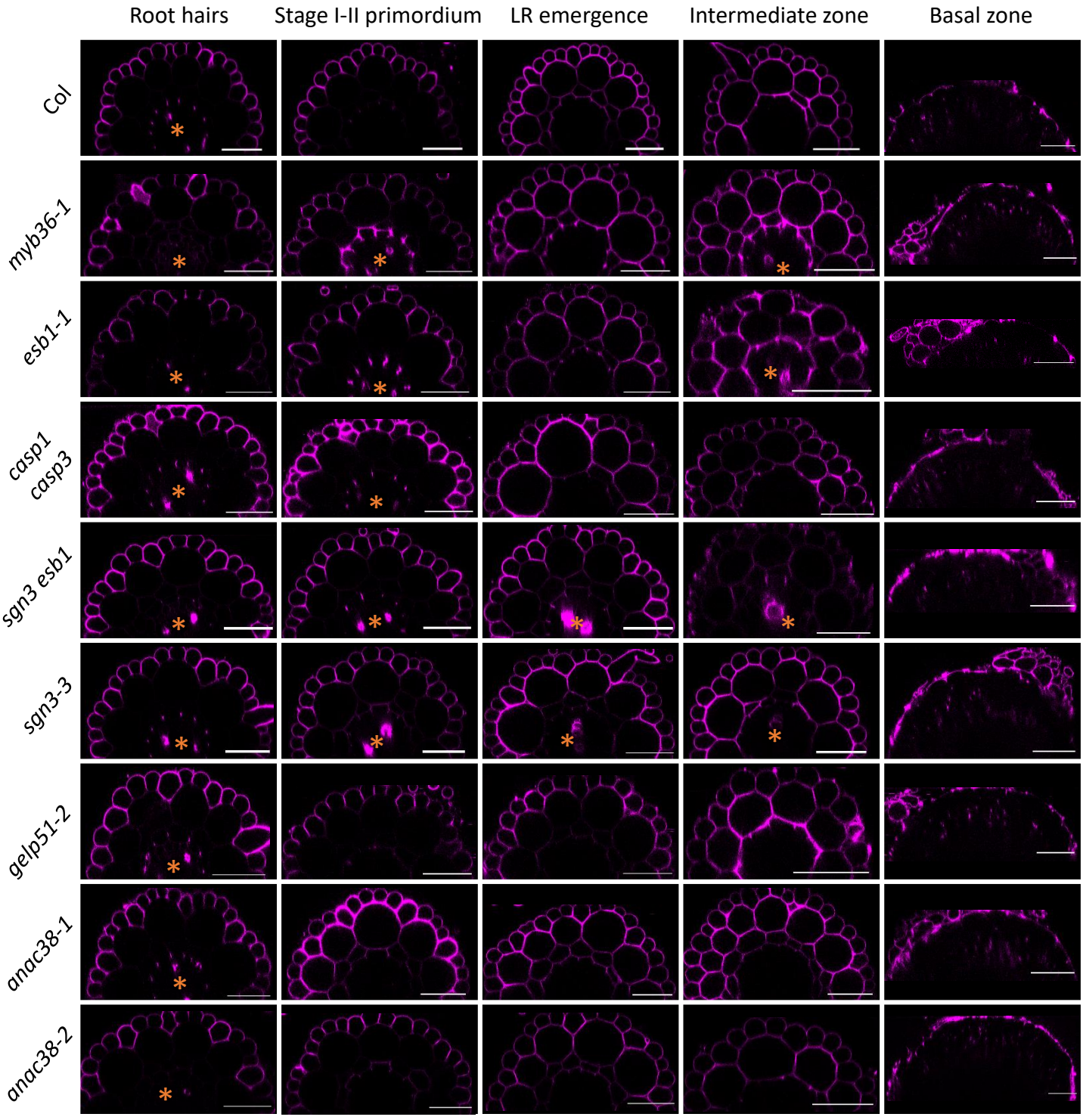

PRIMARY ROOT (continued)

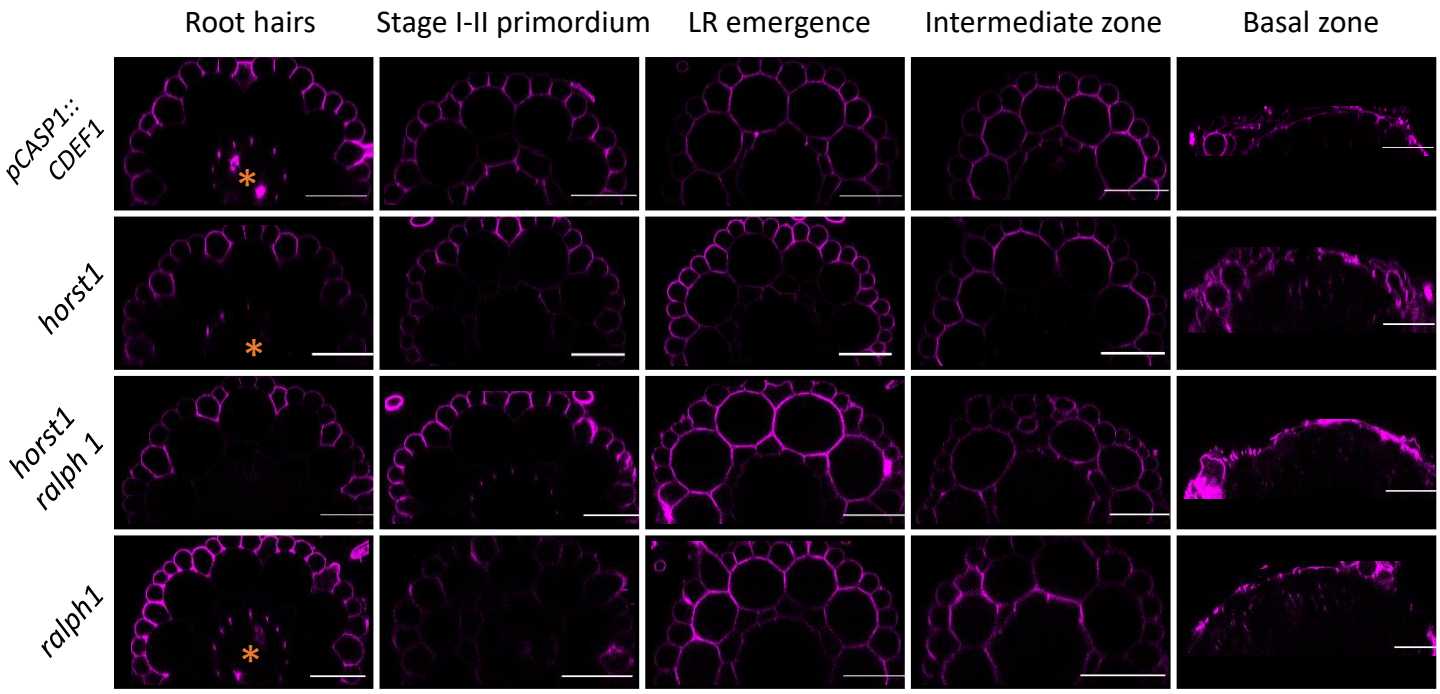

SECONDARY ROOT

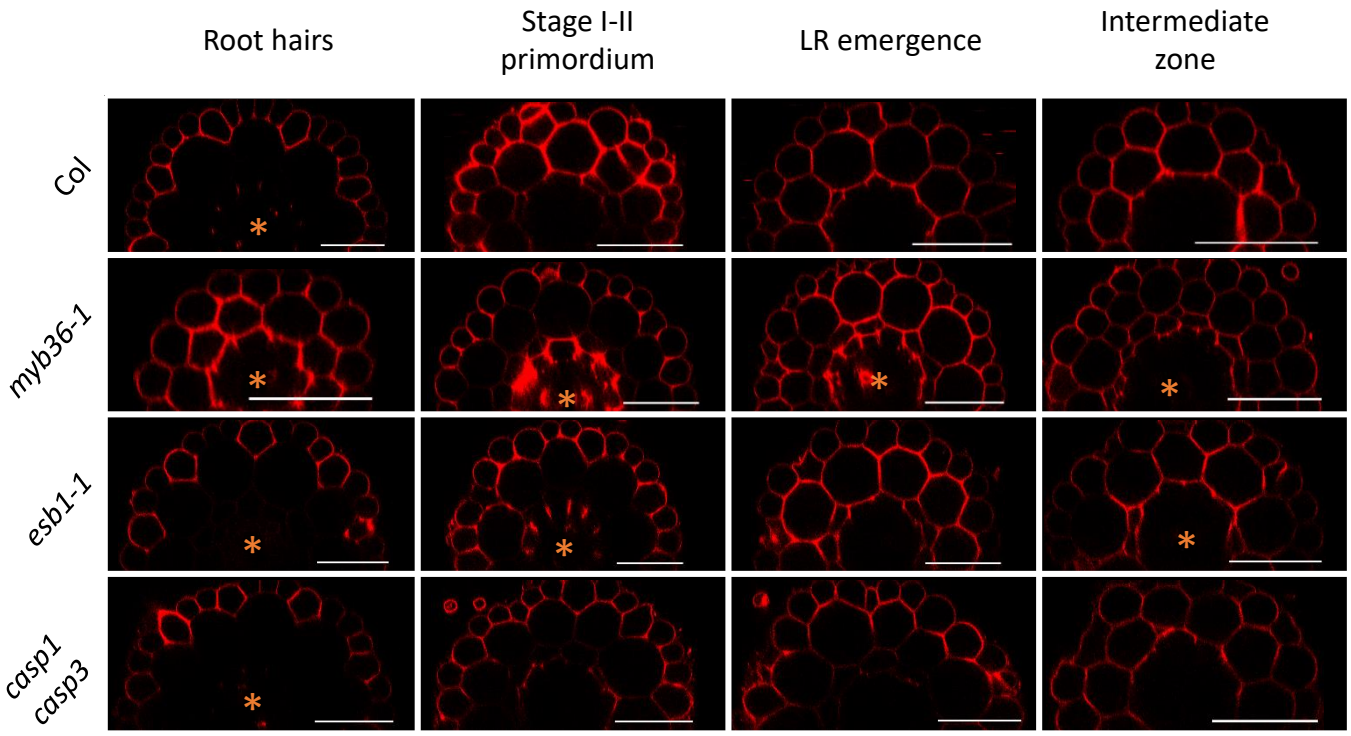

SECONDARY ROOT (continued)

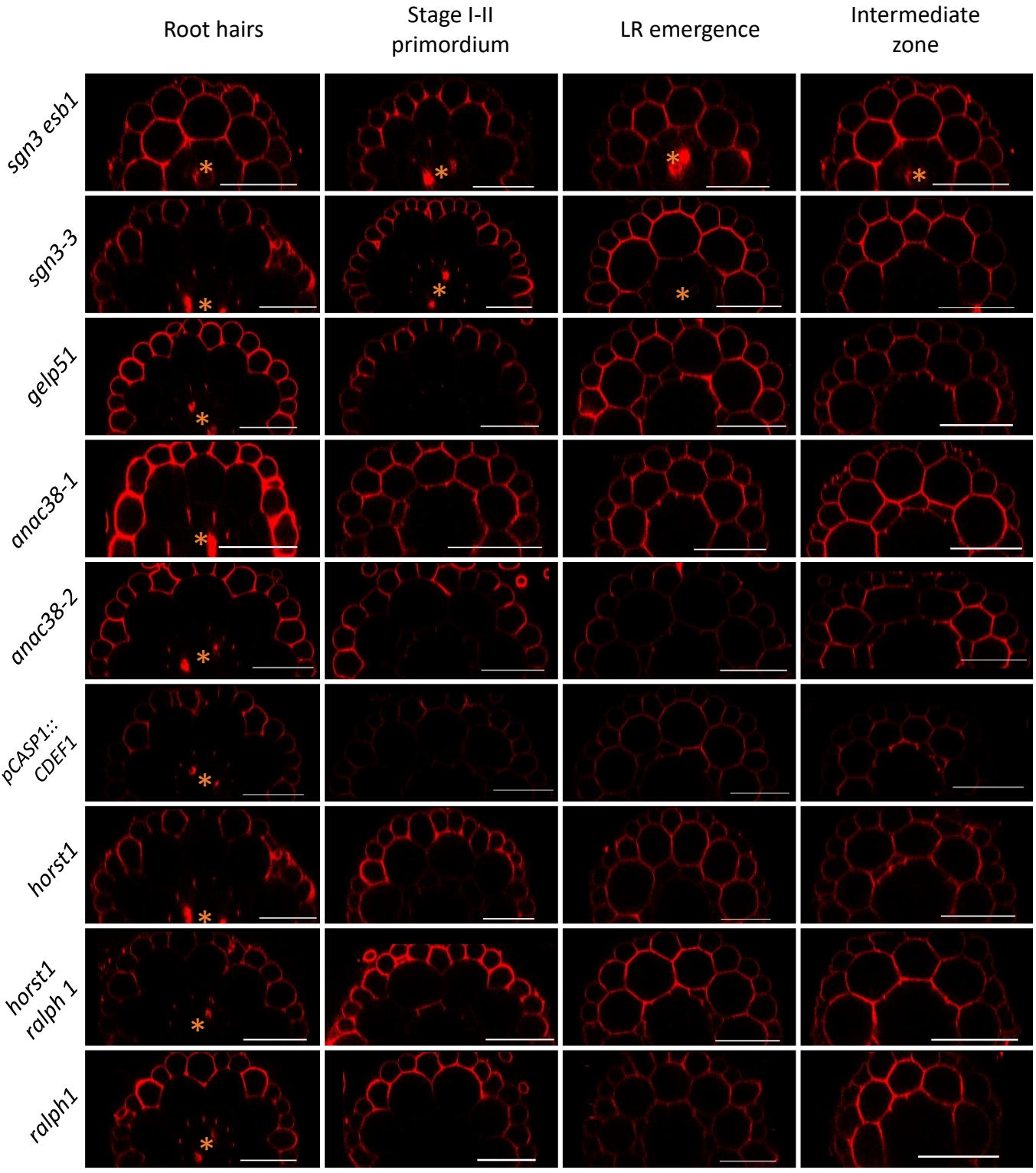

Fig. S3 Deconvolution of the Auramine O signal in 21d hydroponically grown plants enables the detection and quantification of endodermal and peridermal suberin

a) and b) Reconstitution of a full primary root image of a 21d Arabidopsis Col-0 plant grown for 10 days in vitro and 11 days in hydroponic solution, then stained with Auramine O staining, as in Ursache et al., 2018. Image from 44 tiles taken with a stereo-microscope under bright-field light (a) or under UV-light using the GFP filters (b). Lateral roots longer than ~1cm were severed in order to facilitate the observation of the primary root. Scale bar: 10 mm. In b), suberin developmental stages are indicated following the deconvolution of the Auramine O signal explained below.

c) Close-ups from b) showing the various patterns of Auramine O signal, from the root tip to the base. Xylem vessels are marked with an asterisk while the signal attributed to suberin is highlighted by arrowheads. The outlines of suberin are presented in the panel below each picture. Scale bar: 100µm
No suberin: the signal originates only from the xylem vessels,
Around LRP: besides the xylem vessels, a signal located in the endodermis is visible around the lateral root primordium (LRP) emergence,
Patchy: a signal located in the endodermis is visible but discontinue, xylem vessels can still be observed distinctly,
Continuous: a signal engulfing the stele is observed on top of the xylem vessels. A composite image of this same zone is also shown in i).
Periderm: the auramine O signal covers all the root

d) Confocal observations of the auramine O signal in the stele of roots at the same zones than c). Images were obtained after z-stack reconstitution. Xylem vessels can be distinctly observed and are noted with an asterisk. The pictures confirm the endodermal origin of the other source of signal seen in c), which fill and surrounds the cells. This resembles the staining pattern expected from a suberin lamella covering all endodermal cell surface, very distinct from the band-like, restricted signal in the center of a cell as expected from a lignified Casparian strip. It is highlighted with arrowheads. The outlines of suberin are drawn in the panel below each picture. Scale bar : 50µm

e) Overlay of bright-field and Auramine O signal where epidermal and cortical cells slough off (still visible on the right side). According to Campilho et al. 2020, this position identifies the stage V of periderm development. Scale bar: 100µm

f), g) and h) 3D reconstitution of co-imagings of auramine O and RFP signals from Col plants expressing the suberin synthesis reporter pGPAT5::NLS-RFP construct, in the LRP zone, zone of patchy suberisation, and periderm zone, respectively. A brighter signal in the endodermal cells/periderm cells is associated with the presence of the nuclear RFP signal. In particular, note how a high Auramine O signal is associated to the RFP nuclear localisation on the left side of (f), while almost no signal in both channels occurs on the right side. These observations confirm that the Auramine O signal that can be identified at the endodermis is most probably due to the presence of suberin, and that the patterns observed in (b) can be attributed to the different stages of suberin development.

i) Overlay image of the continuous zone, signals from brightfield and UV/GFP channels. Scale bar: 100µm.

New Phytologist

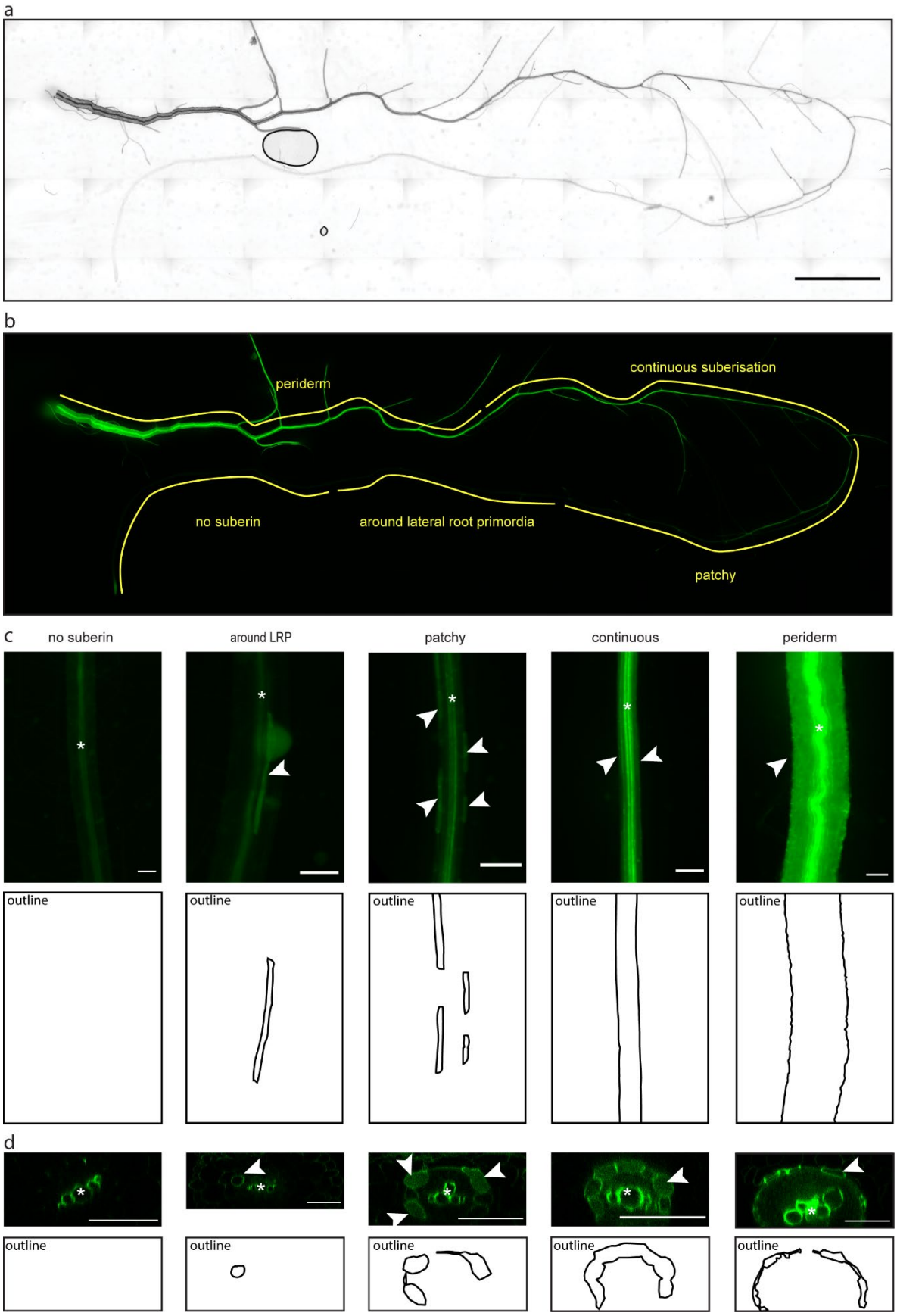

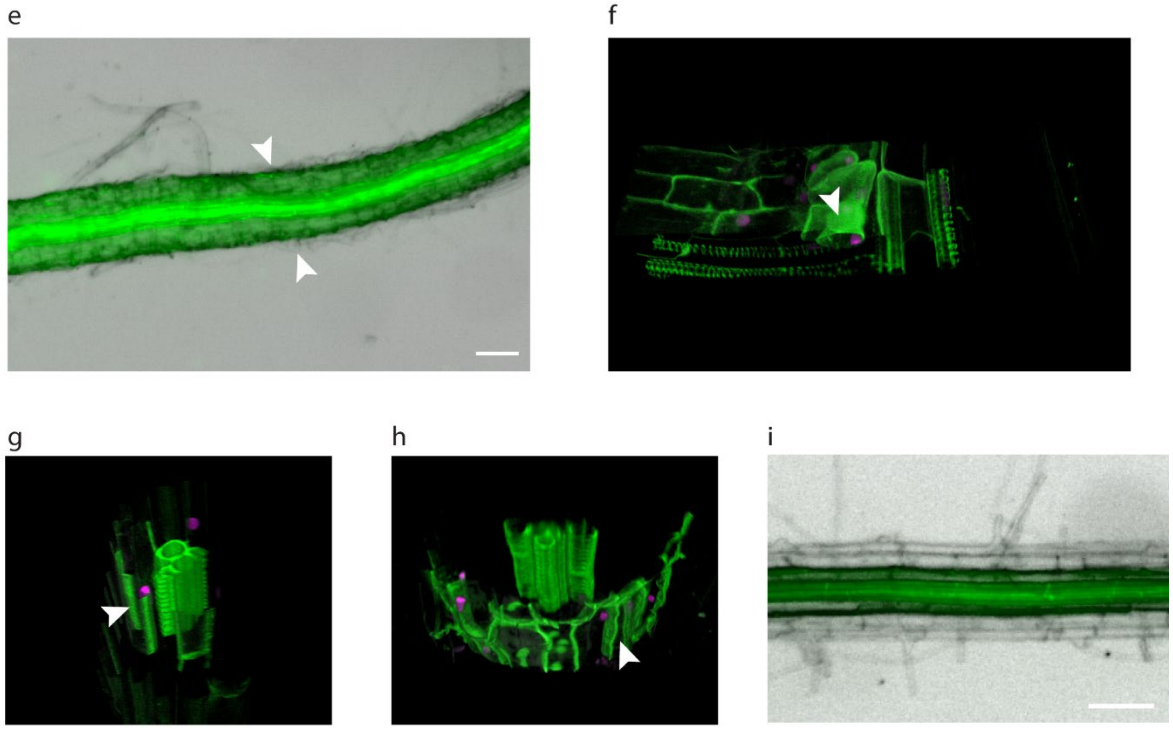
e
f
g
h
i

Fig. S4 Correlations between root hydraulic conductivity ($Lp_{r\text{-}h}$) and PIP aquaporins expression levels in the roots of Col-0 and a collection of 7 Arabidopsis mutants with alterations in endodermal CS and/or suberin. Complement to Fig. 4. Spearman's correlations were not statistically significant. Plants were grown hydroponically for 19-21 days (N=3), color code similar to main figures.

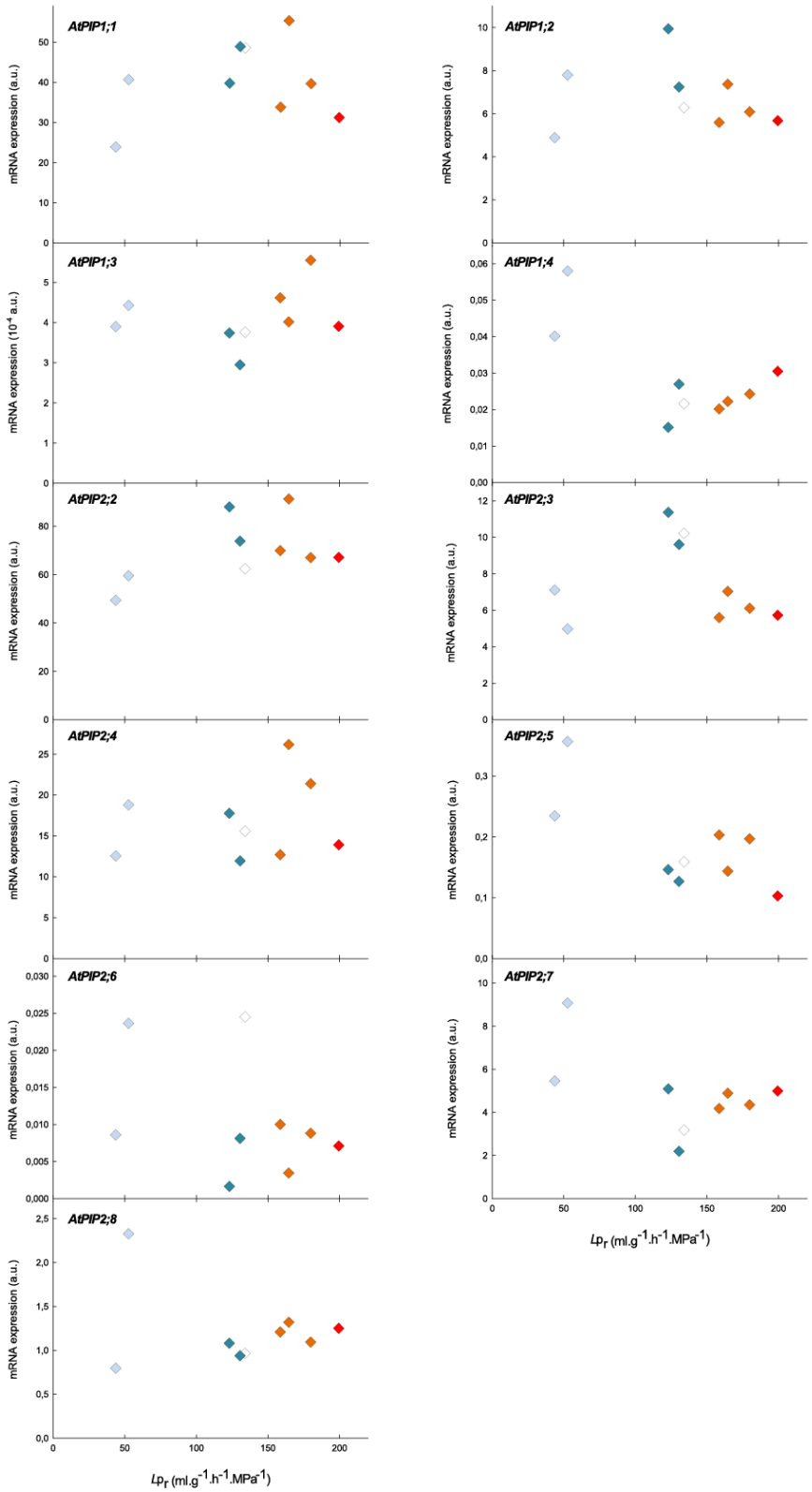

Fig. S5 Effect of NaCl on the root hydraulic conductivity ($Lp_{r\text{-}h}$) of Col-0 and of a collection of 16 CS and suberin mutants. Hydroponically grown 21-day-old Arabidopsis plants were kept untreated (clear bars) or treated for 1h with 100mM NaCl (hashed bars) before measurement using pressure chambers (means ± SE, n=15-20, N=3). Stars over the bars indicate significant differences among control and salt treatment means (* $\alpha < 0.05$; ** $\alpha < 0.01$; *** $\alpha < 0.001$).

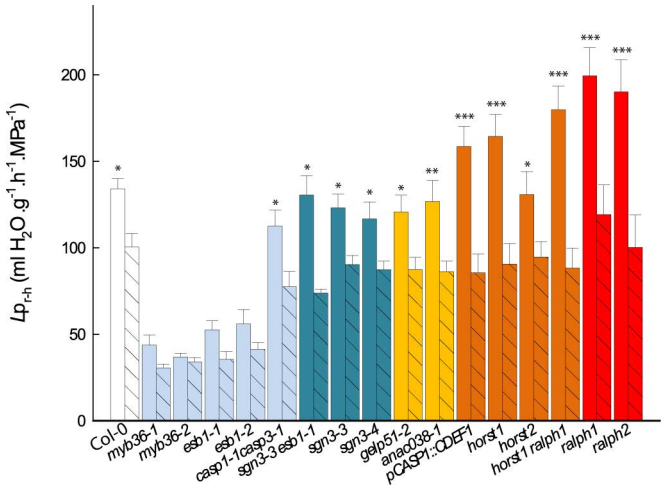

Fig. S6 Kinetics of rosette development and transpiration rates in Col-0 and in a selection of CS and suberin mutants grown under environmentally controlled conditions. Plants were grown in soil in a Phenopsis platform, (a) kinetic of rosette development and (b) day (clear bars) and night (hashed bars) transpiration rates of five-weeks old plants.

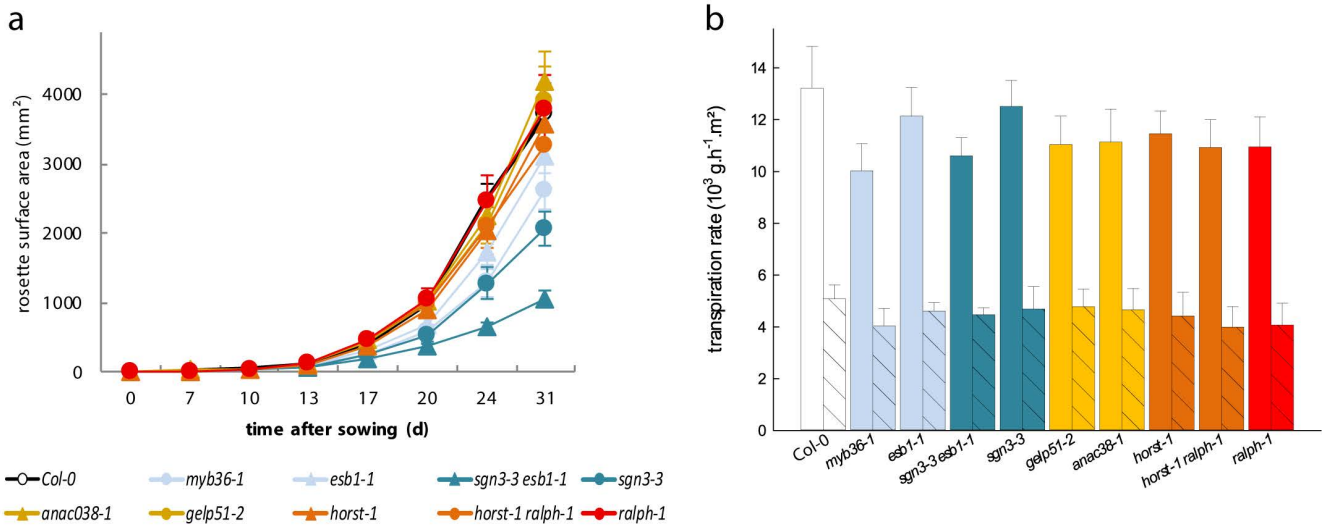

Table S1 Table summarizing the different mutants analyzed in the present study. *Arabidopsis thaliana* genotypes used in this study, grouped and color-coded according to the results presented in Figure 1 and Figures S2 and S3. All mutant genotypes are in the Col-0 background.

Plant	Original accession	Type of mutation	AGI mutated	Reference	Function	Group
Columbia-8 / Col-0	N60000					
myb36-1	11250, lwc1	Fast neutron promoter mutation	AT5G57620	Kamiya et al., 2015	Transcription factor	**CS(-)Sub(+)**
myb36-2	GK-543B11	T-DNA insertion				
esb1-1	14501, dir10	Fast neutron 1 kb promoter deletion	AT2G28670	Baxter et al., 2009	Dirigent domain containing protein	
esb1-2	GABI_858D03	T-DNA insertion				
casp1-1 casp3-1	SAIL_265_H05/ SALK_011092	T-DNA insertions	AT2G36100/ AT2G27370	Roppolo et al., 2011	Casparian strip membrane domain proteins	
sgn3-3	SALK_043282	T-DNA insertion	AT4G20140	Pfister et al. 2014	Leucine-rich repeat transmembrane-type receptor kinase	**CS(-)Sub(=)**
sgn3-4	SALK_064029	T-DNA insertion		Tsuwamoto et al., 2008		
sgn3-3 esb1-1				Wang, Calvo-Polanco et al. 2019		
anac038-1	SALK_103716	T-DNA insertion	AT2G24430	Present work	Transcription factor	**CS(=)Sub(+)**
anac038-2	WiscDsLox_HS007-11H	T-DNA insertion		Present work		
gelp51-2	GK_016A11	T-DNA insertion	AT2G23540	Present work	GDSL-likeLipase /Acylhydrolase	
horst-1	SALK_107454	T-DNA insertion	AT5G58860	Höfer et al., 2008	Cytochrome P450 monooxygenase, CYP86A1	**CS(=)Sub(-)**
horst-2	SALK_104083	T-DNA insertion				
pCASP1::CDEF1		T-DNA insertion		Naseer et al., 2012	Member of the GDSL lipase/esterase family	
horst-1 ralph-1				Present work		
ralph-1	SM.37066	Transposon insertion	AT5G23190	Compagnon et al., 2009	Cytochrome P450 monooxygenase, CYP86B2	**CS(=)Sub(x)**
ralph-2	SALK130265	T-DNA insertion				

Table S2 Ionomic comparisons of the shoots of CS and suberin deficient mutants.

(a) Heat map showing the positive (red), negative (green), or no (grey) differences among each mutant with respect to Col-0 under control conditions. (b) t-test p-values showing significant differences at α=0.05, with respect to Col-0, in the content of each element and for each mutant (n.s., not significant.).

a

Element	*myb36-1*	*esb1-1*	*sgn3-3 esb 1-1*	*sgn3-3*	*gelp51-2*	*anac038-1*	*horst-1*	*horst-1 ralph-1*	*ralph-1*
K									
Fe									
Na									
Mg									
Mn									
Zn									
Ca									
P									
Cu									

b

Element	Treatment	*myb36-1*	*esb1-1*	*sgn3-3 esb 1-1*	*sgn3-3*	*gelp51-2*	*anac038-1*	*horst1*	*horst1 ralph1*	*ralph1*
K	Control	0.0003	<.0001	<.0001	0.0001	n.s.	n.s.	n.s.	n.s.	n.s.
Fe	Control	n.s.	n.s.	0.0370	n.s.	n.s.	n.s.	n.s.	n.s.	n.s.
Na	Control	n.s.	n.s.	<.0001	n.s.	n.s.	n.s.	n.s.	n.s.	n.s.
Mg	Control	0.0002	n.s.	<.0001	<.0001	n.s.	n.s.	n.s.	n.s.	n.s.
Mn	Control	n.s.	n.s.	n.s.	n.s.	n.s.	n.s.	n.s.	n.s.	n.s.
Zn	Control	n.s.	n.s.	<.0001	0.0038	n.s.	n.s.	n.s.	n.s.	n.s.
Ca	Control	0.008	0.0005	n.s.	n.s.	n.s.	n.s.	n.s.	n.s.	n.s.
P	Control	n.s.	n.s.	n.s.	n.s.	n.s.	n.s.	n.s.	n.s.	n.s.
Cu	Control	n.s.	n.s.	n.s.	n.s.	n.s.	n.s.	n.s.	n.s.	n.s.

References

Baxter I, Hosmani PS, Rus A, Lahner B, Borevitz JO, Muthukumar B, Mickelbart MV, Schreiber L, Franke RB, Salt DE. 2009. Root Suberin Forms an Extracellular Barrier That Affects Water Relations and Mineral Nutrition in Arabidopsis. *PLoS Genet* **5**: e1000492.

Campilho A, Nieminen K, Ragni L. 2020. The development of the periderm: the final frontier between a plant and its environment. *Current Opinion in Plant Biology* **53**: 10–14.

Compagnon V, Diehl P, Benveniste I, Meyer D, Schaller H, Schreiber L, Franke R, Pinot F. 2009. CYP86B1 Is Required for Very Long Chain ω-Hydroxyacid and α,ω-Dicarboxylic Acid Synthesis in Root and Seed Suberin Polyester. *Plant Physiology* **150**: 1831–1843.

Franke R, Briesen I, Wojciechowski T, Faust A, Yephremov A, Nawrath C, Schreiber L. 2005. Apoplastic polyesters in Arabidopsis surface tissues – A typical suberin and a particular cutin. *Phytochemistry* **66**: 2643–2658.

Hofer R, Briesen I, Beck M, Pinot F, Schreiber L, Franke R. 2008. The Arabidopsis cytochrome P450 CYP86A1 encodes a fatty acid ω-hydroxylase involved in suberin monomer biosynthesis. *J. Exp. Bot.* **59**: 2347–2360.

Kamiya T, Borghi M, Wang P, Danku JMC, Kalmbach L, Hosmani PS, Naseer S, Fujiwara T, Geldner N, Salt DE. 2015. The MYB36 transcription factor orchestrates Casparian strip formation. *Proceedings of the National Academy of Sciences* **112**: 10533–10538.

Mustroph A, Zanetti ME, Jang CJH, Holtan HE, Repetti PP, Galbraith DW, Girke T, Bailey-Serres J. 2009. Profiling translatomes of discrete cell populations resolves altered cellular priorities during hypoxia in Arabidopsis. *Proceedings of the National Academy of Sciences* **106**: 18843–18848.

Naseer S, Lee Y, Lapierre C, Franke R, Nawrath C, Geldner N. 2012. Casparian strip diffusion barrier in Arabidopsis is made of a lignin polymer without suberin. *Proceedings of the National Academy of Sciences* **109**: 10101–10106.

Pfister A, Barberon M, Alassimone J, Kalmbach L, Lee Y, Vermeer JE, Yamazaki M, Li G, Maurel C, Takano J, *et al.* 2014. A receptor-like kinase mutant with absent endodermal diffusion barrier displays selective nutrient homeostasis defects. *eLife* **3**: e03115.

Roppolo D, De Rybel B, Tendon VD, Pfister A, Alassimone J, Vermeer JEM, Yamazaki M, Stierhof Y-D, Beeckman T, Geldner N. 2011. A novel protein family mediates Casparian strip formation in the endodermis. *Nature* **473**: 380–383.

Tsuwamoto R, Fukuoka H, Takahata Y. 2008. GASSHO1 and GASSHO2 encoding a putative leucine-rich repeat transmembrane-type receptor kinase are essential for the normal development of the epidermal surface in Arabidopsis embryos. *The Plant Journal* **54**: 30–42.

Ursache R, Andersen TG, Marhavý P, Geldner N. **2018**. A protocol for combining fluorescent proteins with histological stains for diverse cell wall components. *The Plant Journal* **93**: 399–412.

Wang P, Calvo-Polanco M, Reyt G, Barberon M, Champeyroux C, Santoni V, Maurel C, Franke RB, Ljung K, Novak O, *et al.* 2019. Surveillance of cell wall diffusion barrier integrity modulates water and solute transport in plants. *Scientific Reports* **9**: 4227.

Woody ST, Austin-Phillips S, Amasino RM, Krysan PJ. **2006**. The WiscDsLox T-DNA collection: an arabidopsis community resource generated by using an improved high-throughput T-DNA sequencing pipeline. *Journal of Plant Research* **120**: 157–165.